2023 IEEE/ASME International Conference on Advanced Intelligent Mechatronics (AIM)
June 28-30, 2023. Seattle, Washington, USA

Bio-mimetic Autonomous Underwater Vehicle Control Using Time Delayed Estimation Technique

Abdullah Algethami[1], Rajasree Sarkar[2], Syed Muhammad Amrr[3], and Arunava Banerjee[4]

***Abstract*— An autonomous underwater vehicle (AUV) is a crewless robotic vehicle that dives into the water and performs without human assistance. This paper focuses on developing trajectory tracking control for bio-mimetic AUV system under uncertain environments. Therefore, a relatively new control technique called time delay-based estimation control is proposed for trajectory tracking under multiple uncertainties. This algorithm estimates the total disturbance in the system using immediate past information of input and output of feedback state and control variables. The benefit of this scheme is that it avoids assumptions about a priori upper bound information of disturbance. Further, the control structure is simple and does not require any high-frequency switching or high gain to nullify the effects of disturbance. The theoretical analysis of the proposed scheme guarantees the uniformly ultimate bounded stability of the closed-loop system. The numerical analysis is also carried out to validate the control performance of the given algorithm for lemniscate reference path tracking.**

I. INTRODUCTION

Aquatic vertebrates are capable of moving at fast speeds which in turn has drawn the widespread attention of researchers in the field of bio-inspired robotics. This feature has been used for biomimetics, such that the natural capabilities of such vertebrates can be effectively mimicked in human-engineered systems. One such area where such nature-inspired spatial locomotion has been replicated is in autonomous underwater vehicles (AUV). AUVs are being extensively used for underwater surveillance as well as monitoring. However, much improvement was desired to the conventional propeller based locomotion of AUVs, which came in the form of bio-mimicking a fish. Such biomimicked AUVs were found to be quieter, more maneuverable (lesser accidents), and possibly more energy efficient. Merging the conventional rigid body dynamics with the bio fluid dynamics, which reproduces fish-like swimming, a unified model of robotic fish was proposed in [1]–[3]. This robotic fish comprises of its head as the first link followed by the two-link manipulator, which resembles the tail. This tail works as the propeller, which generates the required thrust for the underwater vehicle. The coordinated multi-propulsion kinematic modeling of a biomimetic robotic fish is developed on the Solidworks platform, which is shown in Fig. 1.

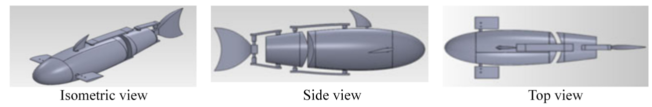

Fig. 1. Bio-mimetic fish model in Solidworks [2].

Various control strategies have been proposed for enhancing the performance of AUVs or bioinspired fish underwater vehicles. Among these schemes, the open-loop strategies [4] have been seen to use both electrostatic and electromagnetic actuators in order to replace the muscles of fish. Fuzzy based methodologies [5], [6] have been used in literature for efficient planar control of the AUV, while Lyapunov functions have been utilized to determine the stability for the vehicle's tracking system. By assuming the impact of vortex shedding along with drift, a control affine methodology was proposed in [7], and a quasi-steady control based on fluid flow was presented in [8] which has the capability of predicting either the forward motion or the turning of the vehicle based on swimming gaits. Also, fish brain mimicking at a very basic level, in order to control the movement of AUV has been explored in [9]. This process utilizes the concepts of central pattern generator along with finite state machine techniques to generate the control input appropriately. In addition to these strategies, the extensive use of motion control strategies can be seen in the state of the art for matching the computational demand of the system by first determining the torque requirement [10] while increasing the freedom of the controller. In this regard, both feed-forward control [11] and computed torque method [7], [10] have been implemented in literature and practice.

In the last few decades, time-delayed control (TDC) methodology [12]–[14] has been widely used for designing control laws for varied system primarily due to its inherent capability of alleviating assumption of bounded uncertainty which is quite conservative for real-time practical systems. Also, this methodology does not require apriori knowledge about the upper bound of uncertainties. The TDC strategy is able to relax these conservative assumptions by considering a relatively non-conservative assumption of slowly varying uncertainties. The unknown part of system dynamics, along with uncertainties, is estimated using the data from prior instant, which in turn introduces a delay in the control formulation, though the system is delay-free. Thus, the technique is termed as time-delayed estimation

[1]A. Algethami is with the Department of Mechanical Engineering, College of Engineering, Taif University, Taif 21944, Saudi Arabia. a_algethami@tu.edu.sa
[2]R. Sarkar is with the Department of Electrical Engineering, Indian Institute of Technology Delhi, New Delhi 110016, India. rajasree.sarkar11@gmail.com
[3]S. M. Amrr is with the Department of Electrical Engineering (ISY), Linköping University, Linköping 58183, Sweden. syedamrr@gmail.com
[4]A. Banerjee is with the Department of Mechanical Engineering, University of Alberta, Edmonton, AB T6G 2R3, Canada. arunavabanerjee27@gmail.com

(TDE). The TDC approach is explored for robot manipulators [15], synchronous motors [16], wheeled mobile robots [17], biped robots [18], shape memory alloys [19], unmanned aerial vehicles [20], missile guidance [21], [22], reusable launch vehicles [23], attitude controller for spacecraft [24], etc. Thus, this work makes use of the TDC robust control strategy to design an efficient control law for the underwater vehicle. The proposed control law demonstrates superior tracking capabilities and is able to guide the vehicle along the reference trajectory, which is an essential aspect for underwater navigation. The TDC based robust control law is also able to effectively tackle the external disturbances and uncertainties affecting the system. Stability analysis has also been included in this work based on Lyapunov analysis which ensures UUB stability. The TDC based strategy has been shown to outperform the widely popular PD controller for the desired objectives.

The rest of the paper is organised as follows: Section II discusses the system model in brief, which is followed by the control law formulation in Section III. The stability analysis is included in Section IV and the results from simulation studies are provided in Section V. Finally, the concluding remarks are presented in Section VI.

II. Model Description

In this work, a three-link manipulator has been designed to work as a bio-inspired robotic fish that operates underwater. The Lighthill (LH) mathematical model [25] is integrated with the kinematic and dynamic model of the robotic fish model for obtaining the tail lateral positions, thus obtaining the unified dynamic model. The shape of the model mimics the structure of a carangiform fish [26]. The head which is also the first link works as a mobile base, with the two other rotational joints connected through caudal tails act as thrusters that use lateral displacement to facilitate motion. The biomechanics of the relative pressure forces have been integrated with that of the moments to ease the undular motion of the AUV.

The robotic fish dynamics model can be mathematically described by the following system of equation [27]

$$\boldsymbol{M}(\boldsymbol{q})\ddot{\boldsymbol{q}} + \boldsymbol{C}(\boldsymbol{q},\dot{\boldsymbol{q}})\dot{\boldsymbol{q}} + \boldsymbol{g}(\boldsymbol{q}) + \boldsymbol{d}(t) = \boldsymbol{\tau}(t) \tag{1}$$

where, $\boldsymbol{q} \in \mathbb{R}^n$ represents the joint position state variable and $\boldsymbol{\tau} \in \mathbb{R}^n$ denotes the control torque. The other parameters governing the evolution of the system dynamics (1) are: the inertia mass matrix $\boldsymbol{M}(\boldsymbol{q},\dot{\boldsymbol{q}}) \in \mathbb{R}^{n\times n}$, the Coriolis centripetal function $\boldsymbol{C}(\boldsymbol{q},\dot{\boldsymbol{q}}) \in \mathbb{R}^{n\times n}$, the gravity vector $\boldsymbol{g}(\boldsymbol{q}) \in \mathbb{R}^n$, and combination of slip force, damping force and friction forces $\boldsymbol{f}(\dot{\boldsymbol{q}}) \in \mathbb{R}^n$. Any external disturbances affecting the system is represented as $d(t)$ [28].

In this paper, a tracking problem has been addressed where a robust controller is to be designed such that the robotic fish system (1) follows a reference positional trajectory $\boldsymbol{q}_r$. In this regard, the joint position error is defined as $\tilde{\boldsymbol{q}} = \boldsymbol{q} - \boldsymbol{q}_r$. Differentiating $\tilde{\boldsymbol{q}}$ with respect to time and then multiplying both sides with $\boldsymbol{M}(\boldsymbol{q})$, gives:

$$\boldsymbol{M}(\boldsymbol{q})\ddot{\tilde{\boldsymbol{q}}} = \boldsymbol{M}(\boldsymbol{q})(\ddot{\boldsymbol{q}} - \ddot{\boldsymbol{q}}_r). \tag{2}$$

By substituting the expression for $\boldsymbol{M}(\boldsymbol{q})\ddot{\boldsymbol{q}}$ as (1) in (2), the error dynamics is formulated as follows:

$$\boldsymbol{M}(\boldsymbol{q})\ddot{\tilde{\boldsymbol{q}}} = \boldsymbol{\tau}(t) - \boldsymbol{C}(\boldsymbol{q},\dot{\boldsymbol{q}})\dot{\boldsymbol{q}} - \boldsymbol{g}(\boldsymbol{q}) - \boldsymbol{d}(t) - \boldsymbol{M}(\boldsymbol{q})\ddot{\boldsymbol{q}}_r. \tag{3}$$

All the functions of states, system uncertainties and external disturbances are lumped together into a single function as $\boldsymbol{N} = [-\boldsymbol{C}(\boldsymbol{q},\dot{\boldsymbol{q}})\dot{\boldsymbol{q}} - \boldsymbol{g}(\boldsymbol{q}) - \boldsymbol{d}(t) - \boldsymbol{M}(\boldsymbol{q})\ddot{\boldsymbol{q}}_r]$. The error dynamics (3) now is expressed as

$$\boldsymbol{M}(\boldsymbol{q})\ddot{\tilde{\boldsymbol{q}}} = \boldsymbol{\tau}(t) + \boldsymbol{N}(\boldsymbol{q},\dot{\boldsymbol{q}},\boldsymbol{q}_r). \tag{4}$$

For the purpose of brevity, the arguments of the functions in (4) are dropped and all parameters being explicit functions of time, $\boldsymbol{M}(\boldsymbol{q})$ and $\boldsymbol{N}(\boldsymbol{q},\dot{\boldsymbol{q}},\boldsymbol{q}_r)$ are henceforth represented as $\boldsymbol{M}(t)$ and $\boldsymbol{N}(t)$ respectively. Thus, (4) now becomes

$$\boldsymbol{M}(t)\ddot{\tilde{\boldsymbol{q}}}(t) = \boldsymbol{N}(t) + \boldsymbol{\tau}(t). \tag{5}$$

III. Controller Design

A. Time-Delayed Control Law

The artificial time-delay philosophy is used in this section, to obtain a stabilizing control law $\boldsymbol{\tau}(t)$ for (5). In this regard, a time-varying design matrix $\bar{\boldsymbol{M}}(t)$ is considered that needs to be appropriately chosen by the designer such that $\bar{\boldsymbol{M}}(t)$ is invertible. Introducing $\bar{\boldsymbol{M}}(t)\ddot{\tilde{\boldsymbol{q}}}$ through adding and subtracting leads to

$$\begin{aligned} &\boldsymbol{M}(t)\ddot{\tilde{\boldsymbol{q}}}(t) + \bar{\boldsymbol{M}}(t)\ddot{\tilde{\boldsymbol{q}}}(t) = \boldsymbol{N}(t) + \bar{\boldsymbol{M}}(t)\ddot{\tilde{\boldsymbol{q}}}(t) + \boldsymbol{\tau}(t) \\ \Rightarrow\ &\bar{\boldsymbol{M}}(t)\ddot{\tilde{\boldsymbol{q}}}(t) = [\bar{\boldsymbol{M}}(t) - \boldsymbol{M}(t)]\ddot{\tilde{\boldsymbol{q}}}(t) + \boldsymbol{N}(t) + \boldsymbol{\tau}(t). \end{aligned} \tag{6}$$

Taking, $\bar{\boldsymbol{N}}(t) = [\bar{\boldsymbol{M}}(t) - \boldsymbol{M}(t)]\ddot{\tilde{\boldsymbol{q}}}(t) + \boldsymbol{N}(t)$, the error dynamics becomes

$$\bar{\boldsymbol{M}}(t)\ddot{\tilde{\boldsymbol{q}}} = \bar{\boldsymbol{N}}(t) + \boldsymbol{\tau}(t). \tag{7}$$

Subsequently, the stabilizing control law for (7) can be designed as:

$$\boldsymbol{\tau}(t) = \bar{\boldsymbol{M}}(t)\boldsymbol{u}(t) - \hat{\boldsymbol{N}}(t), \tag{8}$$

where $\hat{\boldsymbol{N}}(t)$ represents the estimated value of $\boldsymbol{N}(t)$. The auxiliary input $\boldsymbol{u}(t)$ is designed as a closed loop feedback control law as:

$$\boldsymbol{u}(t) = -\boldsymbol{K}_D\dot{\tilde{\boldsymbol{q}}}(t) - \boldsymbol{K}_P\tilde{\boldsymbol{q}}(t), \tag{9}$$

where $\boldsymbol{K}_P$ and $\boldsymbol{K}_D$ are the controller gain parameters. Using (8) and (9), (7) is re-written as:

$$\bar{\boldsymbol{M}}(t)[\ddot{\tilde{\boldsymbol{q}}}(t) - \boldsymbol{u}(t)] = \bar{\boldsymbol{N}}(t) - \hat{\boldsymbol{N}}(t). \tag{10}$$

Multiplying $\bar{\boldsymbol{M}}^{-1}(t)$ on both sides of (10) results in

$$\ddot{\tilde{\boldsymbol{q}}}(t) - \boldsymbol{u}(t) = \bar{\boldsymbol{M}}^{-1}(t)[\bar{\boldsymbol{N}}(t) - \hat{\boldsymbol{N}}(t)] = \boldsymbol{\Lambda}(t) \tag{11}$$

By substituting $\boldsymbol{u}(t)$ as (9) in (11), the closed loop error dynamics for the robotic fish is achieved as:

$$\begin{aligned} &\ddot{\tilde{\boldsymbol{q}}}(t) + K_D\dot{\tilde{\boldsymbol{q}}}(t) + K_P\tilde{\boldsymbol{q}}(t) = \boldsymbol{\Lambda}(t) \\ \Rightarrow\ &\dot{\bar{\boldsymbol{q}}}(t) = \boldsymbol{\mathcal{K}}\bar{\boldsymbol{q}}(t) + \boldsymbol{\phi}(t) \end{aligned} \tag{12}$$

where

$$\bar{\boldsymbol{q}}(t) = \begin{bmatrix}\tilde{\boldsymbol{q}}(t)\\ \dot{\tilde{\boldsymbol{q}}}(t)\end{bmatrix}, \boldsymbol{\mathcal{K}} = \begin{bmatrix}\mathbf{0}_n & \mathbf{I}_n\\ -\boldsymbol{K}_P & -\boldsymbol{K}_D\end{bmatrix}, \boldsymbol{\phi}(t) = \begin{bmatrix}\mathbf{0}_{n\times 1}\\ \boldsymbol{\Lambda}(t)\end{bmatrix}$$

If $\boldsymbol{\phi}(t)$ goes to zero, a suitable choice of the controller gains $\mathcal{K}$ can steer the closed loop system to the origin which leads to ideal tracking of $\boldsymbol{q}_r(t)$. However, $\boldsymbol{\phi}(t)$ represents the estimation error in (12) which appears due to the estimation of the nominal value of $\bar{\boldsymbol{N}}(t)$ by $\hat{\boldsymbol{N}}(t)$. Using (7), $\bar{\boldsymbol{N}}(t)$ is expressed as:

$$\bar{\boldsymbol{N}}(t) = \bar{\boldsymbol{M}}(t)\ddot{\boldsymbol{q}}(t) - \boldsymbol{\tau}(t) \tag{13}$$

The TDE methodology has been employed in this work to carry out the required estimation. The method uses the system dynamics information and input-output measurement data to compute the estimated value $\hat{\boldsymbol{N}}(t)$. One can infer from (13) that an ideal estimation is achieved when $\hat{\boldsymbol{N}}(t)$ is computed by using measurement data of the present time instant t. However, such a requirement indicates availability of control input and other state measurement at that particular instant of time. For practical scenario, such a feat is not admissible and an alternate scheme of using measurement data from previous time instant can be adopted to estimate the effects of uncertainties. Needless to say, one achieves ideal estimation under such philosophy as time difference between current and previous time stamps tends to zero. Representing the previous instant as a time-delayed version of the present instant, the estimated value is expressed as:

$$\hat{\boldsymbol{N}}(t) \approx \bar{\boldsymbol{N}}(t-\gamma) \tag{14}$$

where γ is an artificially induced small time delay representing the difference between the current and previous time instant. It can be seen from (14) that choosing a small enough value of time-delay γ, leads to smaller estimation error $\boldsymbol{\phi}(t)$. In real-time applications, the smallest time realizable is the sampling interval of the processor. Hence, the time-delay is conservatively set equal to the processor sampling time. Thus, the time-delayed version of (13) is subsequently expressed as:

$$\hat{\boldsymbol{N}}(t) \approx \bar{\boldsymbol{N}}(t-\gamma) = \bar{\boldsymbol{M}}(t-\gamma)\ddot{\boldsymbol{q}}(t-\gamma) - \boldsymbol{\tau}(t-\gamma) \tag{15}$$

Using (14) and (15) in (8), the control law for closed loop system (12) is derived as:

$$\boldsymbol{\tau}(t) = \bar{\boldsymbol{M}}(t)\boldsymbol{u}(t) - \bar{\boldsymbol{M}}(t-\gamma)\ddot{\boldsymbol{q}}(t-\gamma) + \boldsymbol{\tau}(t-\gamma) \tag{16}$$

It is to be noted that the original system (12) is inherently free of any time-delay. However, because of the application of time-delayed control scheme, a time-delay of γ is introduced into the system, from where the method derives its name of *'artificial time-delayed control'*.

IV. Stability Analysis

This section discusses the stability of the closed-loop structure of the error system (12) as the proposed TDC control law (16) is applied while taking the following assumption into consideration.

Assumption 1: For the error dynamics (7),

1) Uncertainties in the lumped function $\bar{\boldsymbol{N}}(t)$ varies slowly with time t [18], [24], [29].
2) Variation in the feedback auxiliary input $\boldsymbol{u}(t)$ in between two sampling instants, i.e., γ, is bounded.

Lemma 1: With Assumption 1 being satisfied, the estimation error $\boldsymbol{\Lambda}(t)$ of the closed loop system (12) remains bounded under the application of time-delayed estimation (14) and control law (16) , if there $\exists\ \bar{\boldsymbol{M}}(t)$ such that

$$\left\|\boldsymbol{M}^{-1}(t)\bar{\boldsymbol{M}}(t) - \boldsymbol{I}\right\| < 1,\ \forall t \geq 0 \tag{17}$$

Proof: Using (5), the control torque $\boldsymbol{\tau}(t)$ is expressed as

$$\boldsymbol{\tau}(t) = \boldsymbol{M}(t)\ddot{\boldsymbol{q}}(t) + \boldsymbol{N}(t) \tag{18}$$

The above expression, when written for a delayed time instance $(t-\gamma)$, can be represented as

$$\boldsymbol{\tau}(t-\gamma) = \boldsymbol{M}(t-\gamma)\ddot{\boldsymbol{q}}(t-\gamma) - \boldsymbol{N}(t-\gamma) \tag{19}$$

Using (19) in (16), the control law $\boldsymbol{\tau}(t)$ becomes

$$\boldsymbol{\tau}(t) = \bar{\boldsymbol{M}}(t)\boldsymbol{u}(t) - [\bar{\boldsymbol{M}}(t-\gamma) - \boldsymbol{M}(t-\gamma)]\ddot{\boldsymbol{q}}(t-\gamma) - \boldsymbol{N}(t-\gamma) \tag{20}$$

From (11), the estimation error $\boldsymbol{\Lambda}(t)$ at time t is represented as:

$$\boldsymbol{\Lambda}(t) = \ddot{\boldsymbol{q}}(t) - \boldsymbol{u}(t) \tag{21}$$

Multiplying $\boldsymbol{M}(t)$ on both sides gives

$$\boldsymbol{M}(t)\boldsymbol{\Lambda}(t) = \boldsymbol{M}(t)\ddot{\boldsymbol{q}}(t) - \boldsymbol{M}(t)\boldsymbol{u}(t) \tag{22}$$

Substituting $\boldsymbol{M}(t)\ddot{\boldsymbol{q}}(t)$ by using (7) and replacing $\boldsymbol{\tau}(t)$ as (20), the above equation is re-written as

$$\begin{aligned} \boldsymbol{M}(t)\boldsymbol{\Lambda}(t) = {} & [\bar{\boldsymbol{M}}(t) - \boldsymbol{M}(t)]\boldsymbol{u}(t) - [\bar{\boldsymbol{M}}(t-\gamma) \\ & - \boldsymbol{M}(t-\gamma)]\ddot{\boldsymbol{q}}(t-\gamma) + \boldsymbol{N}(t) - \boldsymbol{N}(t-\gamma) \end{aligned} \tag{23}$$

Addition and subtraction of the term $[\bar{\boldsymbol{M}}(t) - \boldsymbol{M}(t)]\boldsymbol{u}(t-\gamma)$ on the right hand side of (23) with small rearrangement gives

$$\begin{aligned} \boldsymbol{M}(t)\boldsymbol{\Lambda}(t) = {} & [\bar{\boldsymbol{M}}(t) - \boldsymbol{M}(t)][\boldsymbol{u}(t) - \boldsymbol{u}(t-\gamma)] \\ & - [\bar{\boldsymbol{M}}(t-\gamma) - \boldsymbol{M}(t-\gamma)]\ddot{\boldsymbol{q}}(t-\gamma) + \boldsymbol{N}(t) \\ & - \boldsymbol{N}(t-\gamma) + [\bar{\boldsymbol{M}}(t) - \boldsymbol{M}(t)]\boldsymbol{u}(t-\gamma) \end{aligned} \tag{24}$$

Exploiting the time-delayed expression of (11) and substituting $\ddot{\boldsymbol{q}}(t-\gamma) = \boldsymbol{u}(t-\gamma) + \boldsymbol{\Lambda}(t-\gamma)$, (24) becomes

$$\begin{aligned} \boldsymbol{M}(t)\boldsymbol{\Lambda}(t) = {} & -[\bar{\boldsymbol{M}}(t-\gamma) - \boldsymbol{M}(t-\gamma)]\boldsymbol{\Lambda}(t-\gamma) \\ & + [\bar{\boldsymbol{M}}(t) - \boldsymbol{M}(t)][\boldsymbol{u}(t) - \boldsymbol{u}(t-\gamma)] - [\bar{\boldsymbol{M}}(t-\gamma) \\ & - \boldsymbol{M}(t-\gamma) - \bar{\boldsymbol{M}}(t) + \boldsymbol{M}(t)]\boldsymbol{u}(t-\gamma) \\ & + [\boldsymbol{N}(t) - \boldsymbol{N}(t-\gamma)] \end{aligned} \tag{25}$$

Recalling that γ is set as the sampling time of the processor in order to ensure better estimation using TDE philosophy. Thus, without loss of generality, the instant t and $(t-\gamma)$ has been represented as p^{th} and $(p-1)^{th}$ sampling instances respectively. This translates (25) to

$$\begin{aligned} \boldsymbol{M}(p)\boldsymbol{\Lambda}(p) = {} & -[\bar{\boldsymbol{M}}(p-1) - \boldsymbol{M}(p-1)]\boldsymbol{\Lambda}(p-1) \\ & + [\bar{\boldsymbol{M}}(p) - \boldsymbol{M}(p)][\boldsymbol{u}(p) - \boldsymbol{u}(p-1)] - [\bar{\boldsymbol{M}}(p-1) \\ & - \boldsymbol{M}(p-1) - \bar{\boldsymbol{M}}(p) + \boldsymbol{M}(p)]\boldsymbol{u}(p-1) \\ & + [\boldsymbol{N}(p) - \boldsymbol{N}(p-1)] \end{aligned} \tag{26}$$

Multiplying $\boldsymbol{M}^{-1}(p)$ on both sides, one obtains

$$\begin{aligned}\boldsymbol{\Lambda}(p) = &-\boldsymbol{\eta}_1(p-1)[\boldsymbol{M}^{-1}(p-1)\bar{\boldsymbol{M}}(p-1) - \boldsymbol{I}]\boldsymbol{\Lambda}(p-1) \\ &+ [\boldsymbol{M}^{-1}(p)\bar{\boldsymbol{M}}(p) - \boldsymbol{I}]\boldsymbol{\eta}_2(p-1) \\ &- \boldsymbol{\eta}_1(p-1)[\boldsymbol{M}^{-1}(p-1)\bar{\boldsymbol{M}}(p-1) - \boldsymbol{I}]\boldsymbol{\eta}_3(p-1) \\ &+ [\boldsymbol{M}^{-1}(p)\bar{\boldsymbol{M}}(p) - \boldsymbol{I}]\boldsymbol{\eta}_3(p-1) + \boldsymbol{\eta}_4(p-1) \quad (27)\end{aligned}$$

where

$$\begin{aligned}\boldsymbol{\eta}_1(p-1) &= \boldsymbol{M}^{-1}(p)\boldsymbol{M}(p-1) \\ \boldsymbol{\eta}_2(p-1) &= \boldsymbol{u}(p) - \boldsymbol{u}(p-1) \\ \boldsymbol{\eta}_3(p-1) &= \boldsymbol{u}(p-1) \\ \boldsymbol{\eta}_4(p-1) &= \boldsymbol{M}^{-1}(p)[\boldsymbol{N}(p) - \boldsymbol{N}(p-1)]\end{aligned}$$

Note that boundedness in the function $\boldsymbol{\eta}_1(p-1)$ can be guaranteed by appropriately choosing $\bar{\boldsymbol{M}}(t)$. On the other hand, Assumption 1 ensures boundedness of the functions $\boldsymbol{\eta}_2(p-1)$, $\boldsymbol{\eta}_3(p-1)$ and $\boldsymbol{\eta}_4(p-1)$. Therefore, the condition that guarantees boundedness in estimation error $\boldsymbol{\Lambda}(p)$ can be stated as:

$$\left\| \boldsymbol{M}^{-1}(p)\bar{\boldsymbol{M}}(p) - \boldsymbol{I} \right\| < 1, \ \forall p \in \mathbb{Z}^+ \quad (28)$$

■

Lemma 1 leads to the following theorem on the stability of the closed loop system.

Theorem 1: Under the application of the feedback control law (16) derived using time-delayed estimation (15), states of the closed-loop error system (5) achieve uniformly ultimately bounded (UUB) stability.

Proof: Consider a Lyapunov candidate as:

$$V = \frac{1}{2}\bar{\boldsymbol{q}}(t)^T \boldsymbol{\Theta} \bar{\boldsymbol{q}}(t) \quad (29)$$

where $\boldsymbol{\Theta}$ represents a positive definite matrix that satisfies the Lyapunov equation

$$\boldsymbol{\mathcal{K}}^T \boldsymbol{\Theta} + \boldsymbol{\Theta}\boldsymbol{\mathcal{K}} = -\boldsymbol{\Lambda} \quad (30)$$

and $\boldsymbol{\Lambda}$ is a user-defined matrix which has to be positive definite. Differentiating (29) with respect to time gives

$$\dot{V} = \frac{1}{2}\bar{\boldsymbol{q}}(t)^T \boldsymbol{\Theta}\dot{\bar{\boldsymbol{q}}}(t) + \frac{1}{2}\dot{\bar{\boldsymbol{q}}}(t)^T \boldsymbol{\Theta}\bar{\boldsymbol{q}}(t) \quad (31)$$

Substituting expression of $\dot{\bar{\boldsymbol{q}}}(t)$ as (12), (31) becomes

$$\begin{aligned}\dot{V} &= \frac{1}{2}\bar{\boldsymbol{q}}(t)^T \boldsymbol{\Theta}[\boldsymbol{\mathcal{K}}\bar{\boldsymbol{q}}(t) + \boldsymbol{\phi}(t)] + \frac{1}{2}[\boldsymbol{\mathcal{K}}\bar{\boldsymbol{q}}(t) + \boldsymbol{\phi}(t)]\boldsymbol{\Theta}\bar{\boldsymbol{q}}(t) \\ &= \frac{1}{2}\bar{\boldsymbol{q}}(t)^T[\boldsymbol{\Theta}\boldsymbol{\mathcal{K}} + \boldsymbol{\mathcal{K}}^T\boldsymbol{\Theta}]\bar{\boldsymbol{q}}(t) + \bar{\boldsymbol{q}}(t)^T\boldsymbol{\Theta}\boldsymbol{\phi}(t) \\ &= -\frac{1}{2}\bar{\boldsymbol{q}}^T(t)\boldsymbol{\Lambda}\bar{\boldsymbol{q}}(t) + \bar{\boldsymbol{q}}^T(t)\bar{\boldsymbol{\xi}}(t) \quad (32)\end{aligned}$$

where $\boldsymbol{\Theta}\boldsymbol{\phi}(t) = \bar{\boldsymbol{\xi}}(t)$. It is to be noted that Lemma 1 ensures boundedness in $\boldsymbol{\phi} = [\boldsymbol{0}_{n\times 1}^T \quad \boldsymbol{\Lambda}^T]^T$. On the other hand, $\boldsymbol{\Theta}$ is an user defined matrix which satisfies the Lyapunov equation (30), subsequently, one can also conclude the $\boldsymbol{\phi} \in \mathcal{L}_\infty$, which indicates that $\boldsymbol{\phi}$ remains bounded for all time. Therefore, the derivative of V in (32) alternately satisfies

$$\begin{aligned}\dot{V} &\leq -\lambda_{\min}(\boldsymbol{\Lambda})\left\|\bar{\boldsymbol{q}}(t)\right\|^2 + \left\|\bar{\boldsymbol{q}}(t)\right\|\left\|\bar{\boldsymbol{\xi}}(t)\right\|, \\ \dot{V} &\leq -\rho\left\|\bar{\boldsymbol{q}}(t)\right\|^2 - [\lambda_{\min}(\boldsymbol{\Lambda}) - \rho]\left\|\bar{\boldsymbol{q}}(t)\right\|^2 + \left\|\bar{\boldsymbol{q}}(t)\right\|\left\|\bar{\boldsymbol{\xi}}(t)\right\| \quad (33)\end{aligned}$$

where the value of the parameter $\boldsymbol{\rho}$ is defined within the bound $0 < \boldsymbol{\rho} < \boldsymbol{\lambda}_{\min}(\boldsymbol{\Lambda})$. Since, the Lyapunov function satisfies $V \leq \frac{1}{2}\boldsymbol{\lambda}_{\max}(\boldsymbol{\Lambda})\left\|\bar{\boldsymbol{q}}(t)\right\|^2$, the above expression is revised as:

$$\begin{aligned}\dot{V} &\leq -\boldsymbol{\lambda}_{\min}(\boldsymbol{\Lambda})\left\|\bar{\boldsymbol{q}}(t)\right\|^2 + \left\|\bar{\boldsymbol{q}}^T(t)\bar{\boldsymbol{\xi}}(t)\right\| \\ &\leq -\bar{\boldsymbol{\rho}}V - [\boldsymbol{\lambda}_{\min}(\boldsymbol{\Lambda}) - \bar{\boldsymbol{\rho}}\left\|\bar{\boldsymbol{q}}(t)\right\|^2 + \left\|\bar{\boldsymbol{q}}(t)\right\|\left\|\bar{\boldsymbol{\xi}}(t)\right\|\end{aligned}$$

where $\bar{\boldsymbol{\rho}} = \frac{2\boldsymbol{\rho}}{\boldsymbol{\lambda}_{\max}(\boldsymbol{\Theta})}$ Note that $\dot{V} \leq -\bar{\boldsymbol{\rho}}V$ if the following condition holds

$$\begin{aligned}[\boldsymbol{\lambda}_{\min}(\boldsymbol{\Lambda}) - \boldsymbol{\rho}]\left\|\bar{\boldsymbol{q}}(t)\right\|^2 &\geq \left\|\bar{\boldsymbol{q}}(t)\right\|\left\|\bar{\boldsymbol{\xi}}(t)\right\| \\ \Rightarrow \left\|\bar{\boldsymbol{q}}(t)\right\| &\geq \frac{\left\|\bar{\boldsymbol{\xi}}(t)\right\|}{[\boldsymbol{\lambda}_{\min}(\boldsymbol{\Lambda}) - \boldsymbol{\rho}]} \quad (34)\end{aligned}$$

Condition (34) states that for every $t \geq 0$ if the error $\bar{\boldsymbol{q}}(t)$ is outside the region defined by the right-hand side of (34) then $\bar{\boldsymbol{q}}(t)$ exponentially convergences to the same region and remains therein. Thus, the closed-loop system (7) always remains uniformly ultimately bounded. ■

V. Numerical Analysis

This section presents the simulation result of the proposed time delay-based control strategy (16) for the AUV system (1) under the influence of uncertainties and disturbances. The proposed results are also compared with computed torque control with PD compensation (CTC-PD) [2]. The underwater behavior of the AUV in simulation is modeled by (16), which has three linear and three angular position states, namely x, y, z and roll ϕ, pitch θ, yaw ψ, respectively. The model parameters of the AUV are extracted from [27], and the initial conditions are given in Table I. Reference trajectories are also given in Table I, which is selected such that it forms a lemniscate path system scenario. Further, the controller gain parameters for both the schemes are tabulated in Table II. The control gain parameters are tuned based on iterative performance measures while the time delay constant was selected to be greater than the sampling time.

TABLE I
AUV Parameters

Description	Value
Initial position	$[0.05,\ 0.4,\ 0.1, -0.5, -0.1, -0.4]$
Initial velocity	$[0,\ 0,\ 0,\ 0,\ 0,\ 0]$
Ref. trajectory	$\boldsymbol{q}_r = \begin{bmatrix} 0.4(\sin(0.3t)) \\ 0.6(\sin(0.6t)) \\ 0.3(\sin(0.6t)) \\ 0.2(\sin(0.5t)) \\ 0.3(\sin(0.4t)) \\ 0.4(\sin(0.7t)) \end{bmatrix}$

TABLE II
Control Parameters

Schemes	Parameters
TDE (16)	$K_D = 12$, $K_P = 18$, $\gamma = 1 \times 10^{-3}$s
CTC-PD	$K_v = 30$, $K_p = 20$

To ensure the resilience of the proposed control scheme against system uncertainties and disturbances, the nominal parameters of the AUV are selected as 80% of the true values. Further, the external disturbance is considered as $\boldsymbol{d} = -0.3\dot{\boldsymbol{x}} - 0.3\textbf{sign}(\boldsymbol{x}) + 0.3\sin(0.3t)$, where $\boldsymbol{x} \in \mathbb{R}^6$ is the system states [30].

A. Simulation Results Discussion

The simulation performance of the proposed strategy and the comparative scheme are shown in Fig 2–6. Figure 2 presents the 3-dimensional trajectory tracking response in x-y-z plane for both control techniques. It can be observed from this 3-dimensional plot that the proposed TDE scheme tracks the lemniscate reference path more effectively than the CTC-PD scheme. The above observation can easily be realized through tracking error responses, which are illustrated in Fig. 3 and Fig. 4. The linear relative error response $[\tilde{q}_1,\ \tilde{q}_2,\ \tilde{q}_3]^T$ in Fig. 3 for the proposed scheme shows that its convergence rate is faster with a better steady-state response. On the other hand, Fig. 4 depicts the linear error response under the comparative scheme that shows unsatisfactory results during both transient and steady-state periods. The wider residual bound of $[\tilde{q}_1,\ \tilde{q}_2,\ \tilde{q}_3]^T$ in Fig. 4 is because the disturbances are not nullified effectively.

Similarly, the angular position error response $[\tilde{q}_4,\ \tilde{q}_5,\ \tilde{q}_6]^T$ are presented in Fig. 5 and Fig. 6. The angular trajectory tracking performance under the proposed algorithm achieves a better convergence time with a decent steady-state precision than [2]. Further, from the error performance in Fig. 5, the controller (16) has adequate resilience towards unknown external disturbances and parametric uncertainties because there are negligible deviations in the steady state, as compared to Fig. 6. It is also evident that the proposed control method transient response and their performance measure is also illustrated in Table III, which depicts the excellence of the designed scheme over [2] in terms of settling time and residual bound. The convergence time of the position tracking error is lesser, and the residual bound is also narrower under the proposed methodology.

TABLE III
PERFORMANCE COMPARISON

Measures	TDE	CTC-PD
Convergence time (s)	7.86	12.16
Linear residual bound	5.99×10^{-4}	6.6×10^{-3}
Angular residual bound	2.53×10^{-4}	7.79×10^{-4}

VI. Conclusion

This work investigated the application of time delay-based estimation control to improve the bio-inspired AUV locomotive motion under unknown uncertainties. The Lyapunov stability theory establishes the UUB convergence of the closed-loop system. The proposed controller ability is investigated by tracking the joint position and velocity. The simulation results demonstrated that it effectively tracks the reference trajectories of different magnitudes and frequencies. Further, the resilience of the proposed algorithm is also tested under uncertain parameters and unknown time-varying disturbance

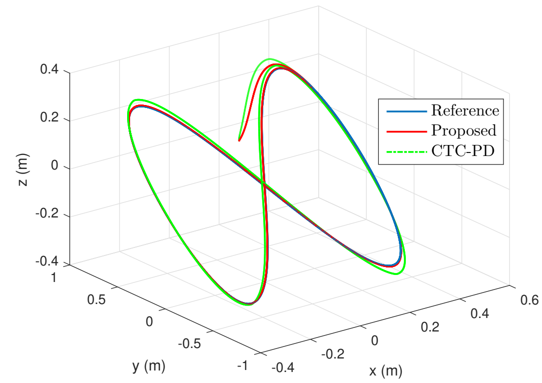

Fig. 2. 3-dimensional trajectory tracking response.

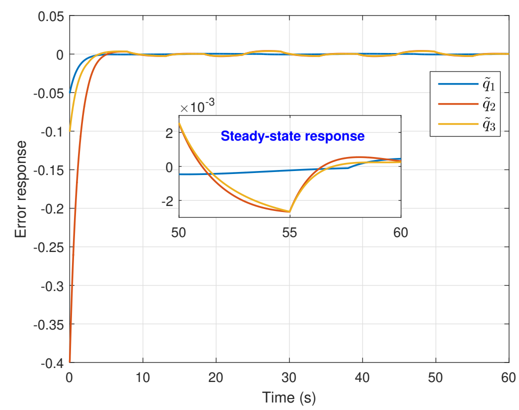

Fig. 3. Linear error response under TDE scheme.

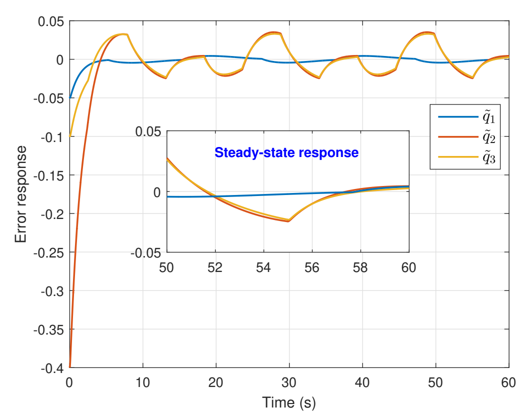

Fig. 4. Linear error response under CTC-PD scheme.

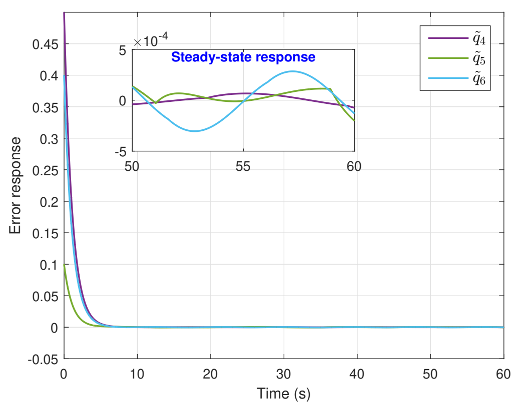

Fig. 5. Angular error response under TDE scheme.

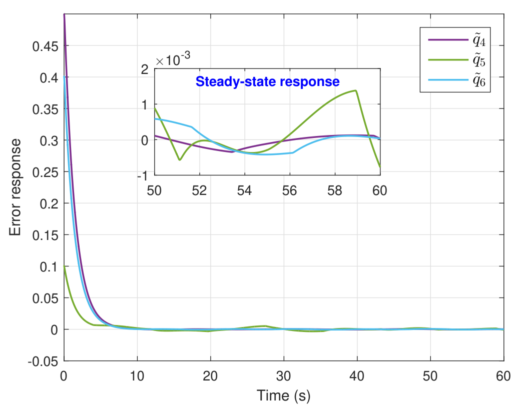

Fig. 6. Angular error response under CTC-PD scheme.

values. The proposed methodology exhibits a substantially improved performance than the CTC-PD algorithm.

References

[1] A. R. Chowdhury, B. Prasad, V. Vishwanathan, R. Kumar, and S. Panda, "Bio-harmonized dynamic model of a biology inspired carangiform robotic fish underwater vehicle," *IFAC Proceedings Volumes*, vol. 47, no. 3, pp. 7258–7265, 2014.

[2] A. R. Chowdhury, S. Sasidhar, and S. K. Panda, "Bio-harmonized control experiments of a carangiform robotic fish underwater vehicle," *Advanced Robotics*, vol. 30, no. 5, pp. 338–351, 2016.

[3] S. Singh, S. Ahmad, S. M. Amrr, S. A. Khan, N. Islam, A. A. Gari, and A. A. Algethami, "Modeling and control design for an autonomous underwater vehicle based on atlantic salmon fish," *IEEE Access*, vol. 10, pp. 97 586–97 599, 2022.

[4] N. Kato, "Control performance in the horizontal plane of a fish robot with mechanical pectoral fins," *IEEE journal of oceanic engineering*, vol. 25, no. 1, pp. 121–129, 2000.

[5] J. E. Colgate and K. M. Lynch, "Control problems solved by a fish's body and brain: A review," *Mechanical Engineering Department, Northwestern University*, 2004.

[6] A. Menozzi, H. A. Leinhos, D. N. Beal, and P. R. Bandyopadhyay, "Open-loop control of a multifin biorobotic rigid underwater vehicle," *IEEE Journal of Oceanic Engineering*, vol. 33, no. 2, pp. 59–68, 2008.

[7] S. D. Kelly and R. M. Murray, "Modelling efficient pisciform swimming for control," *International Journal of Robust and Nonlinear Control*, vol. 10, no. 4, pp. 217–241, 2000.

[8] K. A. Morgansen, V. Duidam, R. J. Mason, J. W. Burdick, and R. M. Murray, "Nonlinear control methods for planar carangiform robot fish locomotion," in *Proceedings of IEEE International Conference on Robotics and Automation (ICRA)*, 2001, pp. 427–434.

[9] A. R. Chowdhury and S. K. Panda, "Finding answers to biological control methods using modulated patterns: An application to bio-inspired robotic fish," in *IEEE International Conference on Robotics and Automation (ICRA)*, 2015, pp. 3146–3153.

[10] H. Berghuis, H. Nijmeijer, and P. Löhnberg, "An addendum on "robust control of robots by the computed torque method"," *Systems & control letters*, vol. 18, no. 5, pp. 403–407, 1992.

[11] T. Kanade, P. K. Khosia, and N. Tanaka, "Real-time control of cmu direct-drive arm ii using customized inverse dynamics," in *23rd IEEE Conference on Decision and Control*, 1984, pp. 1345–1352.

[12] T. C. Hsia and L. Gao, "Robot manipulator control using decentralized linear time-invariant time-delayed joint controllers," in *IEEE Int. Conf. on Robotics and Automation*, 1990, pp. 2070–2075.

[13] T. S. Hsia, T. Lasky, and Z. Guo, "Robust independent joint controller design for industrial robot manipulators," *IEEE transactions on industrial electronics*, vol. 38, no. 1, pp. 21–25, 1991.

[14] K. Youcef-Toumi and O. Ito, "A time delay controller for systems with unknown dynamics," in *Proceedings of 1988 American Control Conference*, 1988, pp. 904–911.

[15] M. Jin, S. H. Kang, and P. H. Chang, "Robust compliant motion control of robot with nonlinear friction using time-delay estimation," *IEEE Trans. on Indust. Electr.*, vol. 55, no. 1, pp. 258–269, 2008.

[16] K.-H. Kim and M.-J. Youn, "A simple and robust digital current control technique of a pm synchronous motor using time delay control approach," *IEEE Trans. Power Electr.*, vol. 16, no. 1, pp. 72–82, 2001.

[17] S. Roy, I. N. Kar, and J. Lee, "Toward position-only time-delayed control for uncertain euler–lagrange systems: Experiments on wheeled mobile robots," *IEEE Robotics and Automation Letters*, vol. 2, no. 4, pp. 1925–1932, 2017.

[18] S. Roy, J. Lee, and S. Baldi, "A new adaptive-robust design for time delay control under state-dependent stability condition," *IEEE Transactions on Control Systems Technology*, 2020.

[19] M. Jin, J. Lee, and K. K. Ahn, "Continuous nonsingular terminal sliding-mode control of shape memory alloy actuators using time delay estimation," *IEEE/ASME Transactions on Mechatronics*, vol. 20, no. 2, pp. 899–909, 2014.

[20] J. Lee, C. Yoo, Y.-S. Park, B. Park, S.-J. Lee, D.-G. Gweon, and P.-H. Chang, "An experimental study on time delay control of actuation system of tilt rotor unmanned aerial vehicle," *Mechatronics*, vol. 22, no. 2, pp. 184 – 194, 2012.

[21] A. Banerjee, J. Mukherjee, M. un Nabi, and I. N. Kar, "An artificial delay based robust guidance strategy for an interceptor with input saturation," *ISA Transactions*, vol. 109, pp. 34–48, 2021.

[22] A. Banerjee, J. Mukherjee, and M. un Nabi, "Time-energy efficient guidance strategy for a realistic 3d interceptor: An adaptive robust time-delayed control approach with input saturation," *Aerospace Science and Technology*, vol. 104, p. 106015, 2020.

[23] R. Sarkar, J. Mukherjee, D. Patil, and I. N. Kar, "Re-entry trajectory tracking of reusable launch vehicle using artificial delay based robust guidance law," *Adv. Space Rese.*, vol. 67, no. 1, pp. 557–570, 2021.

[24] S. M. Amrr, A. Banerjee, and M. Nabi, "Fault-tolerant attitude control of small spacecraft using robust artificial time-delay approach," *IEEE J. Miniat. for Air and Space Sys.*, vol. 1, no. 3, pp. 179–187, 2020.

[25] M. Lighthill, "Note on the swimming of slender fish," *Journal of fluid Mechanics*, vol. 9, no. 2, pp. 305–317, 1960.

[26] P. W. Webb, "Form and function in fish swimming," *Scientific American*, vol. 251, no. 1, pp. 72–83, 1984.

[27] A. N. Ahmad Mazlan, "A fully actuated tail propulsion system for a biomimetic autonomous underwater vehicle," Ph.D. dissertation, University of Glasgow, 2015.

[28] K. S. Fu, R. Gonzalez, and C. G. Lee, *Robotics: Control Sensing. Vis.* Tata McGraw-Hill Education, 1987.

[29] S. M. Amrr, R. Sarkar, A. Banerjee, A. S. Saidi, and M. Nabi, "Fault-tolerant finite-time adaptive higher order sliding mode control with optimized parameters for attitude stabilization of spacecraft," *International Journal of Robust and Nonlinear Control*, vol. 32, no. 5, pp. 2845–2863, 2022.

[30] C. Zhu, L. Jun, B. Huang, Y. Su, and Y. Zheng, "Trajectory tracking control for autonomous underwater vehicle based on rotation matrix attitude representation," *Ocean Engg.*, vol. 252, p. 111206, 2022.